Cotton flooding and drought analysis regarding growth stages in Hubei, China, using a daily agrometeorological index

Long Qian[1], Cheng Chen[2], Xiaohong Chen[1*], Wenzhi Zeng[3], Yawen Gao[3], Kenan Deng[3]

(1. *School of Civil Engineering, Sun Yat-sen University, Guangzhou 510275, China*;
2. *State Environmental Protection Key Laboratory of Environmental Health Impact Assessment of Emerging Contaminatsy, Shanghai 200233, China*;
3. *State Key Laboratory of Water Resources and Hydropower Engineering Science, Wuhan University, Wuhan 430072, China*)

Abstract: Cotton yield is restricted worldwide by flooding and drought that occur across various growth stages. In this study, cotton flooding and drought in Hubei (a major cotton-production province in China) from 1961 to 2019 were analyzed regarding growth stages through a daily index named the standardized antecedent precipitation evapotranspiration index (*SAPEI*). In addition, the impacts of flooding and drought on cotton climatic yield were quantified using multiple regression models. The results showed that the temporal trends of cotton flooding and drought intensities were generally smooth, except for an obvious downward trend for cotton drought intensity at the flowering and boll-forming stage. Additionally, cotton drought intensity varied more drastically than that of flooding over the years. Cotton-flooding proneness was much greater than cotton-drought proneness at all growth stages, and the most flooding-prone and drought-prone periods were identified as the flowering and boll-forming stage and the budding stage, respectively. In terms of spatial distribution, northeastern Hubei and southwestern Hubei were most prone to flooding and drought, respectively. The *SAPEI*-based regression model (R^2=0.490, p<0.001), obviously outperforming the *SPEI*-based model (R^2=0.278, p<0.05), revealed that both cotton flooding and drought exhibited negatively significant effects on cotton climatic yield and that the yield-reducing effect of cotton flooding was much greater than that of drought. Moreover, when growth stages were further considered using regression analysis, only the flowering and boll-forming stage was detected with a significant yield-reducing effect of cotton flooding. In conclusion, the *SAPEI* can effectively assist in monitoring cotton flooding and drought; cotton flooding, especially during the flowering and boll-forming stage and that occurring in northeastern Hubei, is the key issue for cotton field water management in Hubei.

Keywords: irrigation, drainage, climatic yield, waterlogging
DOI: 10.25165/j.ijabe.20231604.6795

Citation: Qian L, Chen C, Chen X H, Zeng W Z, Gao Y W, Deng K N. Cotton flooding and drought analysis regarding growth stages in Hubei, China, using a daily agrometeorological index. Int J Agric & Biol Eng, 2023; 16(4): 173–183.

1 Introduction

Due to increasing climate change, detrimental climatic disasters such as flooding and drought occur more frequently and severely, imposing great impacts on agricultural production[1-3]. As a leading global industrial crop, cotton is confronted with soil waterlogging and water deficit stress worldwide, which are usually induced by flooding and drought[4-9]. Therefore, it is of vital significance to assess the patterns and impacts of flooding and drought occurring during cotton growth periods (hereafter referred to as cotton flooding and drought). From the perspective of natural disaster assessment, the overall impacts of cotton flooding and drought are jointly determined by the characteristics of flooding and drought, as well as by the vulnerability of cotton[10,11]. Thus, it is suggested to jointly investigate the patterns of cotton flooding and drought, as well as the resulting response of cotton yield[12]. In addition, it should also be noted that either the intensities of cotton flooding and drought or the response of cotton yield varies with growth stages. Therefore, the growth-stage effect is an important factor to be considered in evaluating the impacts of cotton flooding and drought.

To quantify the intensities of flooding and drought at the regional level, numerous meteorological indices have been proposed and applied. Since both flooding and drought result from uneven distributions of precipitation, many precipitation-based indices are extensively used, e.g., precipitation concentration degree (*PCD*), *Z* index, and standardized precipitation index (*SPI*)[13-15]. Furthermore, more comprehensive indices have also been developed to account for additional factors. For instance, derived from the *SPI*, the *SPEI* (standardized precipitation and evapotranspiration index) is a currently popular index that considers the effects of air temperature and solar radiation by including the potential evapotranspiration term[16]; this index was originally established for monitoring drought[17], and its applications have been extended to flooding conditions in recent years[12,17,18]. Since agriculture is an important sector that is vulnerable to flooding and drought, numerous researchers have employed meteorological indices such as *SPI* and *SPEI* to assess the impacts of regional flooding and drought on the climate-induced yield fluctuations of various crops, including rice[19], maize[20-22], wheat[23-25], soybean[11],

Received date: 2021-05-31 **Accepted date:** 2023-02-11
Biographies: **Long Qian**, PhD, Associate Researcher, research interest: agricultural drought and flood disasters, Email: qianlong@mail.sysu.edu.cn; **Cheng Chen**, PhD, Associate Engineer, research interest: agricultural drought and flood disasters, Email: chen@saes.sh.cn; **Wenzhi Zeng**, PhD, Associate Professor, research interest: agricultural drought and flood disasters, Email: zengwenzhi1989@whu.edu.cn; **Yawen Gao**, MS Candidate, research interest: agricultural water management, Email: gaoyawen@whu.edu.cn; **Kenan Deng**, MS Candidate, research interest: agricultural water management, Email: KNDeng@whu.edu.cn.
***Corresponding author: Xiaohong Chen**, PhD, Professor, research interest: water resources planning. School of Civil Engineering, Sun Yat-sen University, Guangzhou 510275, China. Tel: +86-20-84115901, Email: eescxh@mail.sysu.edu.cn.

and cotton[12]. These investigations have usually been at monthly or longer time scales; as a result, crop growth stages have often been disregarded or directly assessed at a monthly scale. Nevertheless, when flooding and drought research is confined to crops, short-term events are noteworthy because they can be fatal to crops. Cotton is very sensitive to flooding stress[26], and a flooding event lasting 2-5 d in fields can result in significant cotton yield losses[27,28]. For cotton drought stress, although relevant investigations have primarily focused on long-term drought, previous experimental studies have also indicated that short-term cotton drought lasting 6-10 d can impose a significant reduction in cotton yields[9,27]. Given these concepts, the monthly scale assessment of flooding and drought may be biased because of the offset between short-term events such as flooding and drought within a month. Therefore, more detailed research at short time scales is necessary for precisely assessing the characteristics of cotton flooding and drought at different growth stages.

The responses of cotton yield to flooding and drought have been widely investigated but always through field experiments. To develop reasonable irrigation and drainage schedules in cotton fields, numerous scholars have experimentally explored the quantitative relationships between the intensities of flooding and drought stress and the resulting cotton yield for a single growth stage or multiple growth stages[4,9,12,28,29]. Nevertheless, these field experiments have been performed under controlled growth conditions, differing from the natural conditions under which many factors can jointly affect cotton yield. In this regard, few relevant attempts have been made at the regional level. In fact, in the field of crop responses to water stress, regional-level analysis can be an important supplement for field experimental studies because the latter often lacks practicalities[12,30]. Therefore, in addition to conducting cotton field experiments under various flooding and drought treatments, it is also meaningful to reveal the potential relationships between the intensities of regional flooding and drought and the climate-induced cotton yield, especially emphasizing the growth-stage effect by using short-time-scale indices, as described above.

China is the largest cotton-consuming country and the second-largest cotton-production country in the world, contributing approximately 30% of global cotton production[31]. The Yangtze River basin is one of the three cotton-producing regions in China (the other two are the Yellow River basin and the northwest inland area)[32]; in this region, Hubei Province produces more than 30% of the total cotton yields and thus ranks as the top cotton-producing province (according to the provincial cotton yield data collected from China statistical yearbooks over the past 20 years). Due to the severely uneven distribution of annual precipitation, cotton plants in Hubei are objectively confronted with both flooding and drought problems[27,29]. Studying the patterns and impacts of cotton flooding and drought in Hubei Province can provide valuable guidance for reducing cotton flooding and drought disaster risks. Recently, derived from the popular *SPEI*, a novel agrometeorological index named the standardized antecedent precipitation evapotranspiration index (*SAPEI*) has been established to describe daily drought and flooding conditions[33,34]. This index is calculated in daily steps and accounts for the influence of antecedent soil moisture, which makes it an excellent choice for characterizing cotton flooding and drought at different growth stages. Hence, the aims of the present work were (1) to introduce the *SAPEI* in describing the intensities of cotton flooding and drought at different cotton growth stages in Hubei from 1961 to 2019 and (2) to explore the relationships between the intensities of cotton flooding and drought and the cotton climatic yield.

2 Materials and methods

2.1 Study region and data sources

Hubei Province is a central province in China with an area of 1.859 00×10^5 km^2 (Figure 1). According to China statistical yearbooks over the past 20 years, Hubei has the greatest cotton production among the provinces in the Yangtze River Plain (one of the three cotton-production bases in China), contributing over 30% of the total cotton yield in this region. During the critical growth periods of local cotton plants, rainstorms frequently occur and induce severe flooding problems in cotton fields; in addition, due to the increasingly uneven distribution of precipitation, cotton drought events (especially summer droughts) also occur often[27,29]. According to previous regional research on cotton plants in Hubei[12], as well as our experimental experiences obtained from years of cotton field experiments in Hubei, the entire cotton-growing period in Hubei was divided into four major growth stages: seedling stage (from 5-1 to 6-15), budding stage (from 6-16 to 7-10), flowering and boll-forming stage (from 7-11 to 8-31), and boll-opening stage (from 9-1 to 10-30). The following calculation concerning various growth stages complies with this division. Districts producing very little cotton and districts lacking national-level meteorological stations (i.e., Shenlongjia, Shiyan, and Enshi) were excluded from this study. As a result, the vast majority of the districts in Hubei, including Xiangyang, Yichang, Jingmen, Suizhou, Xiaogan, Tianmen, Wuhan, Jingzhou, Xianning, Huanggang, and Huangshi, were selected as the specific study districts (see Figure 1a). In addition, the annual total precipitation and ET_0 averaged across these stations are displayed in Figure 1b. More detailed information (e.g., climatic conditions and cotton production) is available in a previous publication[12].

a. 19 employed national-level meteorological stations

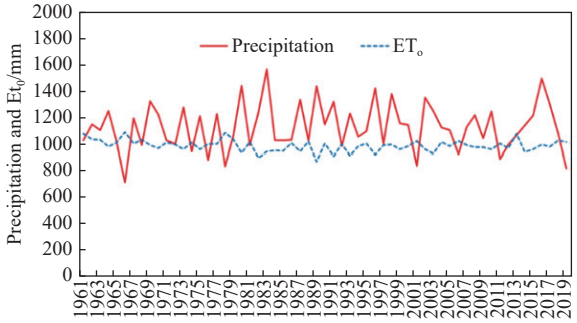

b. Average annual total precipitation and ET_0 of the meteorologicalstations in Hubei from 1961 to 2019

Figure 1 Descriptions of the study region

2.2 Calculation of the *SAPEI*

The *SAPEI* is selected in this study for the following reasons: (1) it is calculated on a daily scale and can capture short-term flooding and drought events; (2) it includes cotton potential evapotranspiration, thus reflecting crop characteristics; and (3) it accounts for the carry effect of previous moisture conditions in the fields. The *SAPEI* originated from the *SPEI*; hence, its calculation is similar to that of the *SPEI*. Specifically, the first step is to compute the difference between precipitation and potential evapotranspiration (*DPE*) in daily steps, describing water surplus or deficit. It is noted that cotton potential evapotranspiration under standard situation (i.e., cotton ET_c), rather than the reference crop potential evapotranspiration under standard situation (i.e., ET_0), was utilized as the potential evapotranspiration term in the *SAPEI*, differing from the calculation of the *SPEI*. As a result, the dynamic water demand special for cotton plants over various growth stages is included in the *SAPEI*. The daily *DPE* can be calculated as:

$$DPE_i = P_i - ET_{c,i} \tag{1}$$

$$ET_{c,i} = k_c \cdot ET_{0,i} \tag{2}$$

where, P_i, $ET_{c,i}$, and $ET_{0,i}$ indicate the precipitation (mm), cotton potential evapotranspiration (mm), and reference crop potential evapotranspiration (mm) on day i, respectively. As indicated by Equation (2), ET_c in this study was calculated with the single crop coefficient method[35]. k_c is the crop coefficient of cotton varying with growth stages. The FAO has provided a set of recommended k_c values for cotton plants, and these values were adjusted to our study region based on local climatic and crop data, including plant height, wind speed, and relative humidity[36]. For the calculation of ET_0, this work employed the widely used Penman-Monteith method because of its solid physical bases and integrated consideration of various factors[36].

After computing daily *DPE*, the carry effect of previous moisture status was accounted for by calculating the antecedent precipitation and evapotranspiration difference (*ADPE*):

$$ADPE_i = \sum_{i=0}^{m} (k^i \cdot DPE_i) \tag{3}$$

where, k^i is an attenuation coefficient to quantify the carry effect of precipitation on day i; and m is the number of forward days. According to previous research, m and k were experientially set to 100 and 0.955, respectively[34].

The final process was to obtain *SAPEI* values from the *ADPE* series, which is the same as deriving *SPEI* values from the monthly *DPE* series (i.e., monthly precipitation minus monthly ET_0)[16]. Specifically, the probability density distribution of a three-parameter log-logistic function F(x) was employed to fit the *ADPE* series over the study period; then, the *SPAEI* was obtained from the standardized values of F(x). A more detailed description of computing the *SAPEI* can be found in previous literature[33,34].

After obtaining *SAPEI* values, the flooding and drought conditions for cotton on each day can be quantified. According to previous research[33,34], *SAPEI* < –0.5 and *SAPEI* > 0.5 referred to cotton drought and flooding conditions, respectively.

2.3 Quantifying cotton flooding and drought intensity over a specific period

As inspired by the widely used waterlogging index SEW_{30}[37], the excessive *SAPEI* (relative to the threshold for flooding or drought) over a given period was accumulated to describe the overall conditions of flooding and drought. This index was defined as the sum of excessive *SAPEI* (i.e., *SESAPEI*).

(1) For flooding (i.e., *SAPEI* > 0.5):

$$SESAPEI_{FL} = \sum_{i=1}^{n} (SAPEI_i - 0.5) \tag{4}$$

(2) For drought (i.e., *SAPEI* < –0.5):

$$SESAPEI_{DR} = \sum_{i=1}^{n} (|SAPEI_i| - 0.5) \tag{5}$$

where, $SESAPEI_{FL}$ and $SESAPEI_{DR}$ indicate the intensity of flooding and drought over a given period, respectively. n is the number of calculation period days. The critical *SAPEI* values for identifying flooding and drought were 0.5 and –0.5, respectively.

As stated previously, in this study, the four major cotton growth stages were from the beginning of May to the end of October; thus, the monthly *SPEI* can also describe the overall flooding or drought conditions across the entire cotton growth period. Similar to the establishment of the *SESAPEI*, the *SESPEI* (i.e., sum of excessive *SPEI*) was calculated based on the monthly *SPEI*.

(1) For flooding (i.e., *SPEI* > 0.5):

$$SESPEI_{FL} = \sum_{j=1}^{m} (SPEI_j - 0.5) \tag{6}$$

(2) For drought (i.e., *SPEI* < –0.5)

$$SESPEI_{DR} = \sum_{j=1}^{m} (\left|SPEI_j\right| - 0.5) \tag{7}$$

where, m is the number of calculation months. In this work, since cotton-growing months were from May to October, m equaled 6. According to previous research that employed the *SPEI* to quantify flooding and drought[24,38,39], the thresholds of the *SPEI* for flooding and drought were set to 0.5 and –0.5, respectively, which were also the same as the employed thresholds of the *SAPEI*.

When describing the proneness of cotton flooding or drought at different growth stages, the duration of each growth stage should be considered. An index that accounts for the durations of each growth stage[12] was employed here:

$$FL_{pr,i} \text{ or } DR_{pr,i} = \frac{SESAPEI_i}{L_i} \tag{8}$$

where, $FL_{pr,i}$ and $DR_{pr,i}$ indicate the flooding proneness and drought proneness of growth stage i, respectively. L_i is the number of days of growth stage i. This index describes the occurrence frequency (i.e., proneness) of flooding and drought at a given period.

In addition, when the FL_{pr} (or DR_{pr}) of different cotton growth stages were compared for various decades, the normalized values would be more comparable[12]:

$$NFL_{pr,i} \text{ (or } NDR_{pr,i}) = \frac{FL_{pr,i}}{\sum_{j=1}^{n} FL_{pr,j}} \times 100\% \left(\text{or } \frac{\mathrm{DR_{pr,i}}}{\sum_{\mathrm{j=1}}^{\mathrm{n}} \mathrm{DR_{pr,j}}} \times 100\% \right) \tag{9}$$

where, $NFL_{pr,i}$ and $NDR_{pr,i}$ are the normalized proneness indices for cotton flooding and drought, respectively (%). n is the number of cotton growth stages.

2.4 Spatial and temporal characteristic analysis

Time series of flooding and drought proneness indices (i.e., $SESAPEI_{FL}$ and $SESAPEI_{DR}$) from 1961 to 2019 were analyzed using the linear trend method[24]:

$$Y_t = k \cdot t + b \tag{10}$$

where, Y_i is the examined meteorological index in year t. k is the

regression coefficient, indicating the changing tendency (upward when $k>0$, downward when $k<0$). In this work, linear trend analysis of the *SESAPEI* was performed for each cotton growth stage. When the linear regression model was significant ($p<0.05$), it indicated that the meteorological index significantly increased ($k>0$) or decreased ($k<0$) with years. The linear regression models were performed by SPSS 12 software (IBM, Amonk, NY); the output values of k, R^2, and p were used to evaluate the changing tendency, regression fit-goodness, and regression significance, respectively.

In addition, to reveal the interannual *SESAPEI* variation at different growth stages, the coefficient of variation (*CV*) was also computed[40].

$$CV_i = \frac{\sigma_i}{\mu_i} \times 100\% \quad (11)$$

where, σ_i and μ_i indicate the standard deviation and mean value of the *SESAPEI* series during decade i, respectively.

For the spatial distribution of cotton flooding and drought, the FL_{pr} and DR_{pr} (Equation 8) of different growth stages and the entire cotton growth period were calculated for each meteorological station in the study region. The results were mapped using ArcGIS 10.2 software (ESRI, Redlands, CA), and the employed interpolation method was inverse distance interpolation.

2.5 Cotton climatic yield

Crop yield can be divided into two parts: the first part is climatic yield, indicating the interannual yield fluctuation induced by climatic factors, such as drought and flooding; the second part is trend yield, which indicates the continuous changing trend of crop yield over time and is determined by various non-climatic factors, e.g., improved agricultural technology. In this study, the annual cotton yields (Y) of the 11 study districts were collected from the latest available series of agricultural statistics from the Hubei Yearbook; thus, 30-year cotton yield data (from 1990 to 2019) were obtained. Then, the cotton trend yield (Y_{tr}, kg/hm^2) was obtained by fitting a quadratic polynomial trend[12,41]. Finally, cotton climatic yield (Y_{cl}, kg/hm^2) was detrended from the actual cotton yield (Y, kg/hm^2) by using the following equation:

$$Y_{cl} = Y - Y_{tr} \quad (12)$$

2.6 Regression analysis of flooding and drought indices *vs.* cotton climatic yield

Multiple linear regression models are powerful tools for revealing the relationships between crop yield and climatic factors, and further predicting regional crop yield[42,43]. Thus, this method was employed to relate the intensities of cotton flooding and drought to the resulting cotton climatic yield. The most basic regression model form can be expressed as:

$$Y_{cl} = k_1 \cdot X_{FL} + k_2 \cdot X_{DR} + m \quad (13)$$

where, X_{FL} and X_{DR} are the flooding and drought indices (i.e., *SESAPEI* and *SESPEI*) over the cotton growth period, respectively. k_1, k_2, and m are regression coefficients. A significant regression model ($p<0.05$) indicates that these drought and flooding variables can significantly explain the variation in cotton climatic yield. Moreover, a negative (positive) k value indicates that the corresponding X variable negatively (positively) affects cotton climatic yield. Therefore, the yield-reducing effects of cotton flooding and drought (when $k<0$) can be quantified by their k values. Furthermore, when Equation (13) was calculated regarding different growth stages, the yield-reducing effects at different growth stages could be compared. When various growth stages were regarded, the regression analysis contained many nonsignificant independent variables; in these cases, the stepwise regression method was employed to defect the best regression models with only significant independent variables. All the abovementioned regression analyses were conducted using SPSS 12 software (IBM, Amonk, NY), which output the regression results, including the values of k, R^2, and p.

3 Results

3.1 Validating the distribution function in the study area

In the calculation of the *SAPEI*, it was first assumed that the *ADPE* series (Equation (3)) complies with a three-parameter log-logistic probability distribution. Hence, this assumption should be validated before applying it to our study region. Four representative districts in Hubei, namely, Huanggang, Jingzhou, Yichang, and Xiangyang, were selected to test the assumed probability distribution function because they are large cotton-production districts and are located with different orientations. Moreover, for each representative district, the interim date of each month during the cotton growth stages (from May to October) was selected as the specific examination example. According to the results of the Kolmogorov–Smirnoff test, D values ranged from 0.07 to 0.10; the corresponding p values ranged from 0.92 to 0.99, which were much greater than 0.05 and demonstrated that the fitness satisfied the significant fitness of the *ADPE* series to the log-logistic distribution in all cases. Figure 2 gives examples of these fitness values by displaying the results on May 15 in the four representative districts. In conclusion, the assumption of a log-logistic distribution for the *ADPE* series was very applicable to our study region.

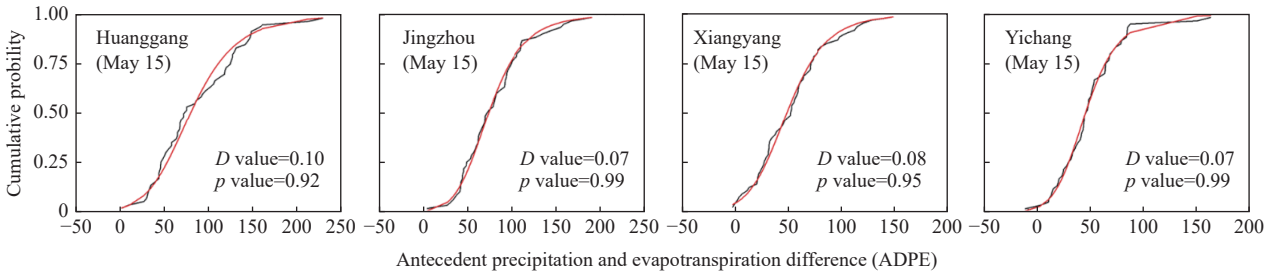

Figure 2 Examples of empirical distribution of the log-logistic distribution (indicated by the black solid line) and theoretical distribution of the *ADPE* series (indicated by the red solid line) in four representative districts

3.2 Temporal trend of cotton flooding and drought over cotton growth stages

The temporal changes in cotton-flooding proneness (FL_{pr}) and drought proneness (DR_{pr}) at the four growth stages and the entire cotton growth period are displayed in Figures 3 and 4. The temporal variation in cotton flooding and drought was not significant at the

growth stages, except that an obvious declining trend (p=0.05) was detected for cotton drought at the flowering and boll-forming stage (Figure 4c). According to the decadal average lines displayed in Figures 3 and 4, the 1980s was the most cotton-flooding prone decade for all the cotton growth stages except the seedling; additionally, the budding stage in the 1960s and the flowering stage in the 1970s witnessed high intensity of cotton drought. Moreover, for each growth stage, the periods with severe cotton flooding (or drought) generally corresponded to slight drought (or flooding). This was a result of the uneven distribution of precipitation within a year.

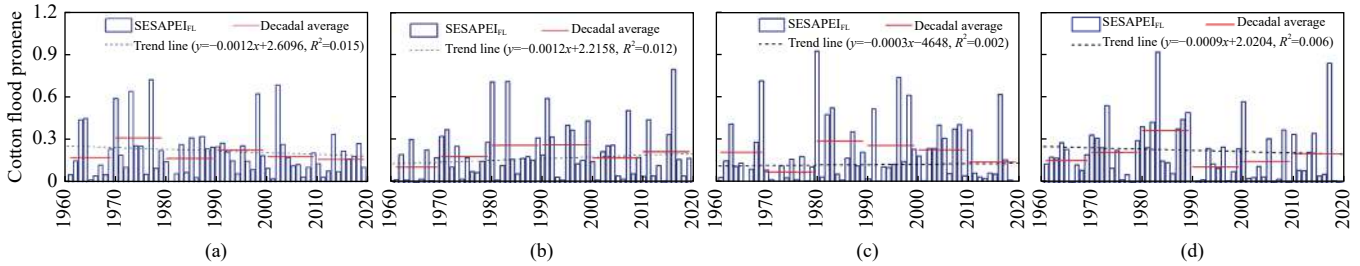

Figure 3 Temporal trend of cotton-flooding proneness during seeding (a), budding (b), flowering and boll-forming (c), and boll-opening (d) from 1961 to 2019. Flooding and drought proneness are represented by the excessive *SAPEI* values divided by the days during the growth stage. Flooding and drought proneness are represented by the excessive *SAPEI* values divided by the days during the growth stage; this information is also applicable to Figures 4, 5, 6, and 7.

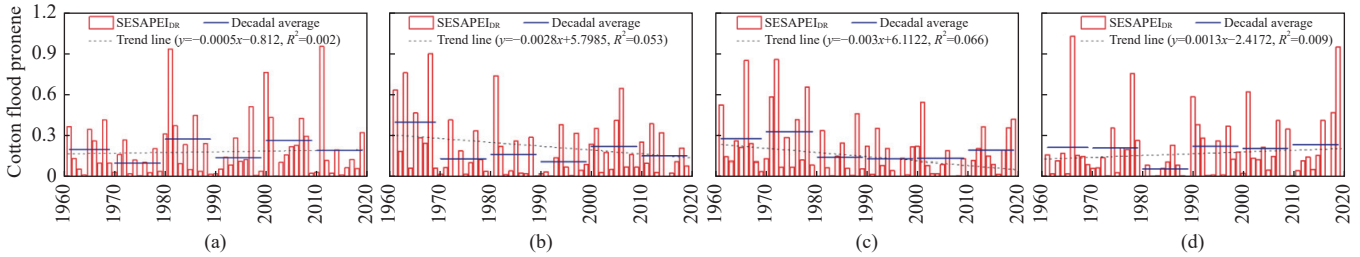

Figure 4 Temporal trend of cotton drought proneness during seeding (a), budding (b), flowering and boll-forming (c), and boll-opening (d) from 1961 to 2019

The variations in cotton flooding and drought differed among decades; thus, we calculated the coefficient of variation (*CV*) of FL_{pr} and DR_{pr} in different decades to quantitatively describe the in-decade temporal variation features of flooding and drought. The results are listed in Tables 1 and 2. Disregarding the differences between decades and growth stages, cotton drought (*CV*=71.27%) was more variable than cotton flooding (*CV*=61.14%). Furthermore, in terms of different decades, cotton-flooding proneness varied most sharply in the latest decade (*CV*=61.91%), while the variation in cotton-drought proneness peaked in the 1980s (*CV*=66.41%). From the perspective of different growth stages, the flowering and boll-forming stage (*CV*=102.34%) and the boll-opening stage (*CV*=116.69%) had the greatest variation in cotton flooding and drought proneness, respectively.

Table 1 Coefficient of variation of the flooding proneness index (FL_{pr}) during different decades

Decade	All stages	Seedling	Budding	Flowering and boll-forming	Boll-opening
1961-1969	59.69	90.23	98.67	96.20	48.58
1970-1979	56.70	73.19	60.37	78.87	74.76
1980-1989	60.57	68.51	90.22	91.67	62.85
1990-1999	53.58	65.37	66.39	92.25	88.71
2000-2009	48.78	98.16	82.38	60.58	122.80
2010-2019	61.91	55.91	107.19	127.20	119.43
1961-2019	61.14	82.03	90.63	102.34	97.48

Table 2 Coefficient of variation of the drought proneness index (DR_{pr}) during different decades

Decade	All stages	Seedling	Budding	Flowering and boll-forming	Boll-opening
1961-1969	69.79	70.74	71.32	87.16	136.96
1970-1979	72.97	85.69	99.29	82.88	100.38
1980-1989	82.05	94.77	133.11	106.70	117.31
1990-1999	55.59	103.90	108.18	85.00	80.38
2000-2009	61.66	81.43	82.63	117.28	89.01
2010-2019	66.41	139.86	80.89	71.44	120.01
1961-2019	71.27	106.87	106.63	101.32	116.69

3.3 Spatial distribution of cotton flooding and drought in Hubei

The spatial distribution of cotton flooding and drought proneness (indicated by FL_{pr} and DR_{pr}) of different growth stages in Hubei are illustrated in Figures 5 and 6. As shown in Figure 5, the spatial distribution of cotton flooding differed sharply between growth stages. For the seedling stage (Figure 5a), there were few flooding-prone areas, and the only high-risk area was the northern part of Xiaogan city (i.e., 'XG' in Figure 5). In comparison, the flooding-prone areas at the budding stage (Figure 5b) were more widespread and were mainly located on the borders of Hubei, especially in southeastern Hubei. Moreover, at the flowering and boll-forming stage, much greater flooding proneness was found (Figure 5c); the flooding-prone areas were numerous and widely distributed across Hubei, and these high-risk areas were adjoined. Finally, the boll-opening stage (Figure 5d) was the period with the least flooding proneness, and the difference between districts was very small. As indicated in Figure 6, the differences in cotton drought proneness between the first three cotton growth stages (Figures 6a-6c) were relatively small, but the boll-opening stage (Figure 6d) had a much lower risk of cotton drought. For the seeding stage (Figure 6a), the drought-prone areas covered the entire middle parts of Hubei. In comparison, at the budding stage,

the drought-prone areas moved to southern Hubei. For the flowering and boll-forming stage, the drought-prone areas were dispersed and more concentrated in eastern Hubei.

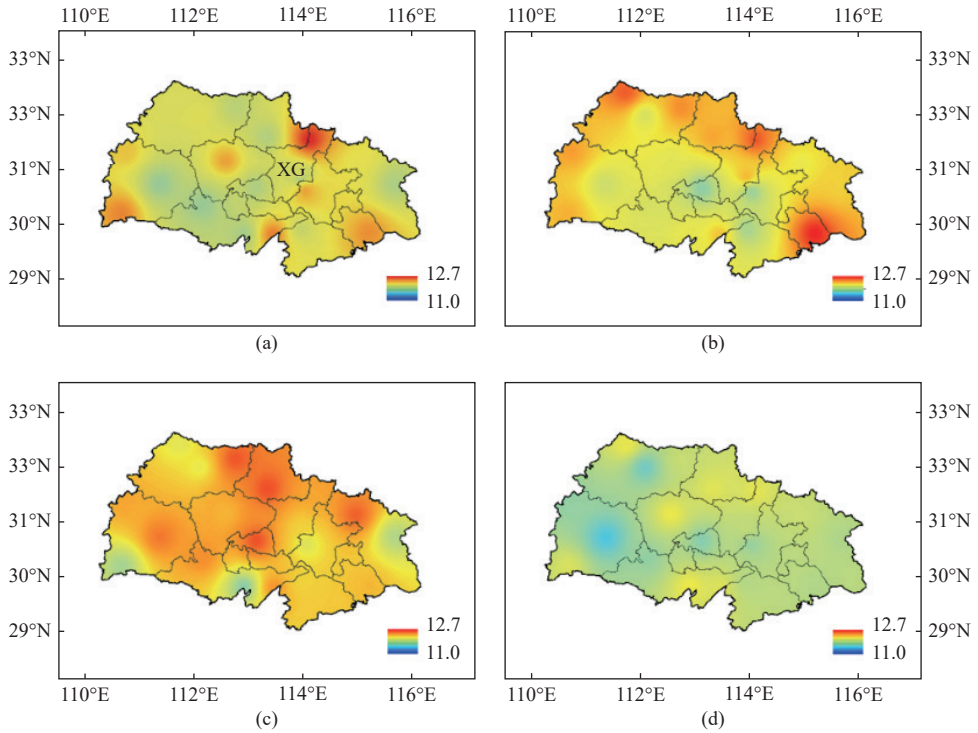

Figure 5 Spatial distribution of cotton-flooding proneness during the seedling (a), budding (b), flowering and boll-forming (c), and boll-opening (d) stages in Hubei. "XG" refers to Xiaogan city

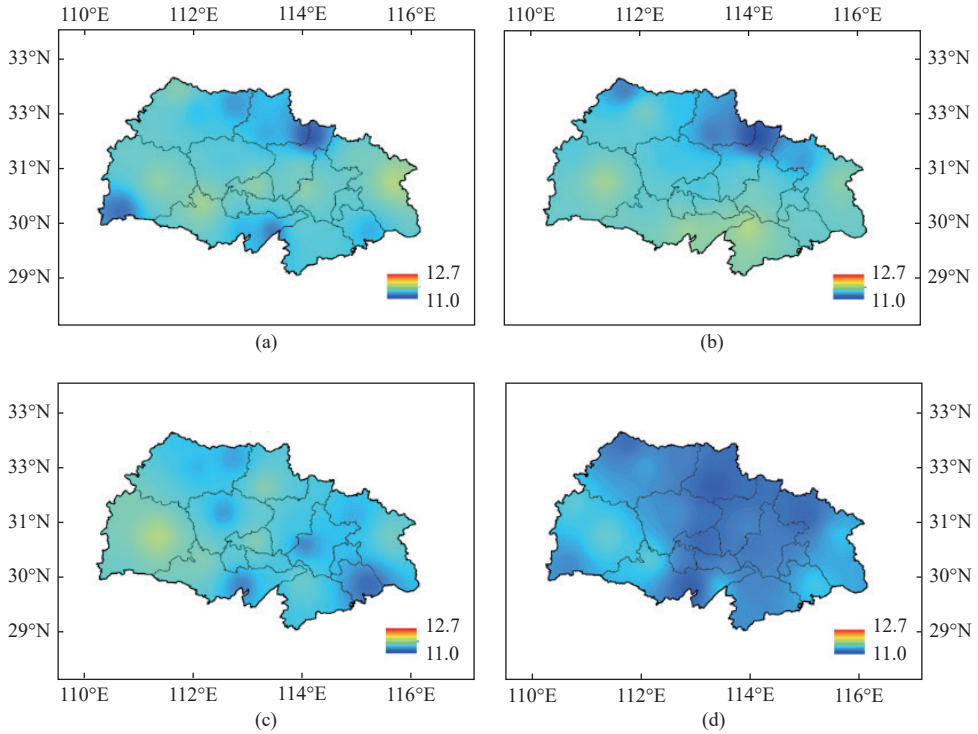

Figure 6 Spatial distribution of cotton-drought proneness during the seedling (a), budding (b), flowering and boll-forming (c), and boll-opening (d) stages in Hubei

Disregarding the differences between growth stages, the spatial distribution of cotton flooding and drought in Hubei is given in Figure 7. The proneness of cotton flooding (Figure 7a) was much greater than that of cotton drought (Figure 7b) in Hubei. The most flooding-prone area was in northeastern Hubei, but this area was at low risk of drought. Similarly, as indicated in Figure 7a, the most drought-prone areas, including southwestern Hubei and eastern Hubei, were at low risk of cotton flooding. Hence, it is concluded that cotton in Hubei was much more prone to flooding than to drought, and the spatial distributions of flooding and drought differed distinctly.

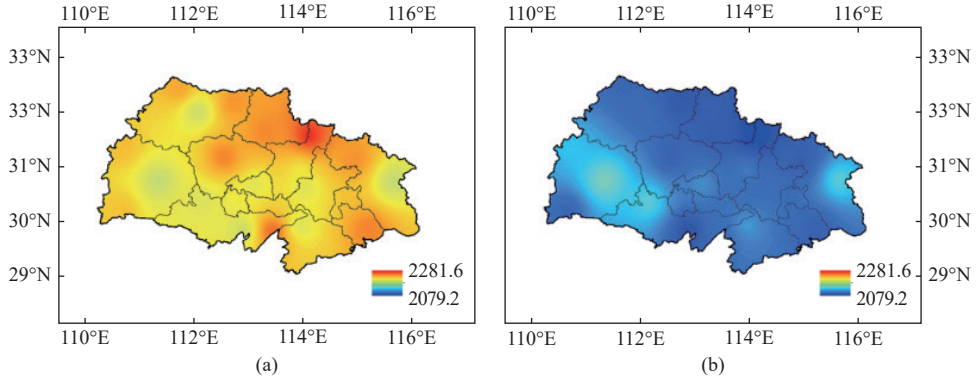

Figure 7 Spatial distribution of cotton-flooding proneness (a) and drought proneness (b) in Hubei

3.4 Relative flooding and drought proneness at different cotton growth stages

To further quantitatively compare the flooding and drought proneness between different cotton growth stages, the normalized proneness indices of flooding and drought (i.e., NFL_{pr} and NDR_{pr} in Equation (9)) were calculated for each decade (see Figure 8).

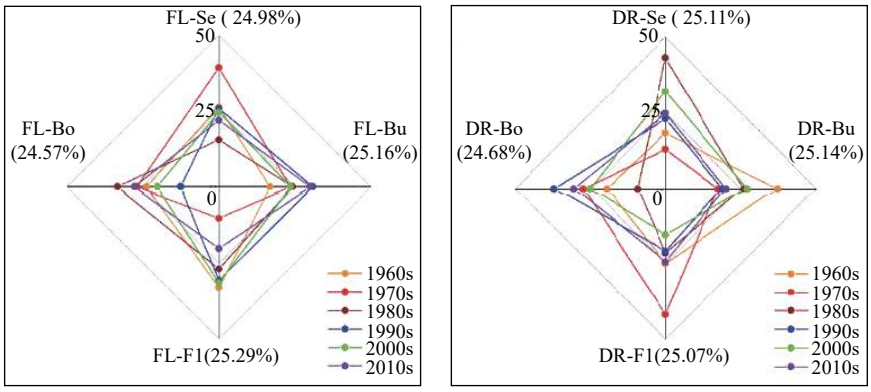

Note: FL and DR represent flooding and drought, respectively. Se, Bu, Fl, and Bo represent the seeding, budding, flowering and boll-forming, and boll-opening stages, respectively. The four percentages in parentheses correspond to the normalized proneness indices over all six decades.

Figure 8 Normalized proneness index of cotton flooding (a) and drought (b) of the four cotton growth stages in the past six decades.

As illustrated in Figure 8, the most flooding-prone stage (or the most drought-prone stage) changed with decades. Moreover, compared with cotton-flooding proneness (Figure 8a), cotton drought proneness (Figure 8b) varied more with growth stages. For instance, the drought proneness at the flowering and boll-forming stage in the 1970s and the drought proneness at the seedling stage in the 1980s were obviously larger than those of other growth stages. From the perspective of growth stages, the flowering and boll-forming stage was generally the most flooding-prone (25.29%, Figure 8a), while the budding stage was the most drought-prone (25.14%, Figure 8b). In comparison, the boll-opening stage had the lowest proneness to both flooding and drought.

3.5 Relationships of the intensities of flooding and drought *vs.* cotton climatic yield

Currently, in China, rain-fed irrigation is still the dominant part of agriculture; thus, field crop yields are primarily affected by flooding and drought[21]. In this study, the potential relationships between the intensities of cotton flooding and drought and cotton climatic yield were explored. The determined regression models are as follows:

(1) For *SESAPEI*:

$$Y_{cl} = -0.586X_{FL} - 0.272X_{DR} + 305.896 \quad (R^2 = 0.490,\ p < 0.001) \quad (14)$$

(2) For *SESPEI*:

$$Y_{cl} = -131.113X_{FL} - 38.603X_{DR} + 190.430 \quad (R^2 = 0.278,\ p < 0.05) \quad (15)$$

where, X_{FL} and X_{DR} are the flooding and drought indices, respectively. ¨ and ˙ indicate that the corresponding X variable is very significant (p<0.01) and significant (p<0.05), respectively.

In terms of the overall model performances, both models passed the significance test; however, the *SAPEI*-based model obviously outperformed the *SPEI*-based model, as demonstrated by a much higher R^2 value and a higher significance level. In addition, judging from the regression coefficients of X_{FL} and X_{DR} in both models, both flooding and drought indices were negatively related to the cotton climatic yield, i.e., the yield-reducing effects of cotton flooding and drought. Nevertheless, the yield-reducing effect of flooding was particularly greater than that of drought: the regression coefficient of the flooding index was much larger than that of the drought index, and only the flooding index was significantly related to cotton climatic yield in both models. Furthermore, considering that the regression models were expected to predict cotton climatic yield at a regional level, the simulated cotton climatic yield using Equations (14) and (15) were compared against the actual cotton climatic yield. The results are displayed in Figure 9. It can be clearly detected that the *SAPEI*-based model (Figure 9a) exhibited a more satisfactory simulation than the *SPEI*-based model, as demonstrated by a lower value in the relative mean absolute error (RMAE), a higher value in the correlation coefficient r, and a linear slope closer to 1.

In addition, to test the conclusion from the above analysis at the district level, further regression analysis was conducted for the 11

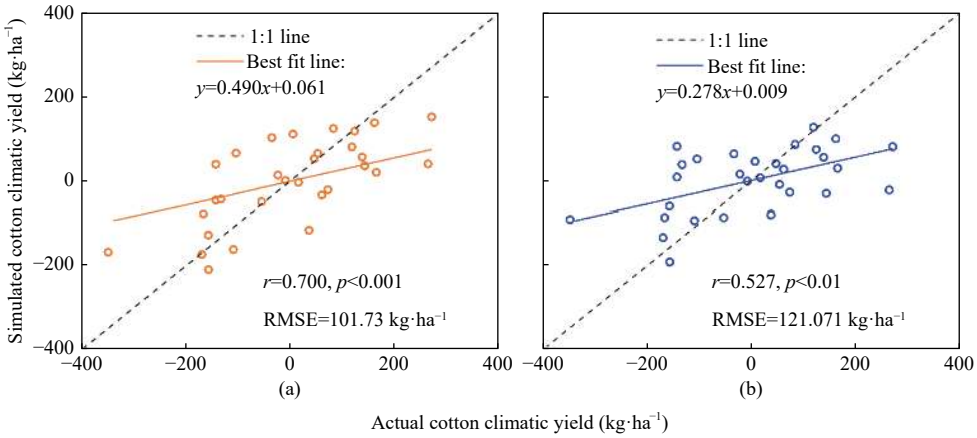

Figure 9 Actual cotton climatic yield *vs.* the simulations using the *SAPEI*-based model (a) and *SPEI*-based model (b)

individual study districts. The number of significant regression results in these districts and the averaged R^2 values are illustrated in Figure 10. Moreover, the regression coefficient results concerning flooding and drought are listed in Table 3.

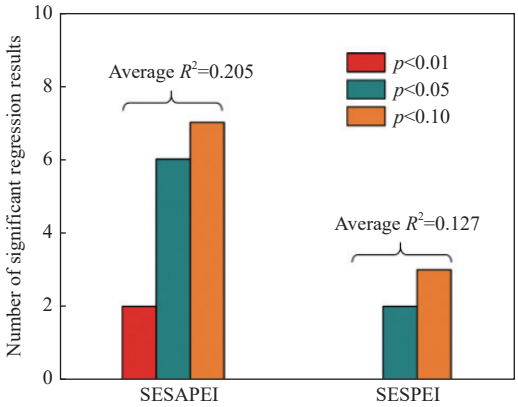

Figure 10 Number of sites with significant regression analytical results. The displayed average R^2 value is the average value of the regression model R^2 in all the study districts.

Table 3 Different performances of cotton flooding and drought in the regression models

Indicators	SESAPEI			SESPEI		
	p<0.01	p<0.05	p<0.10	p<0.01	p<0.05	p<0.10
Number of significant flooding coefficients	1	2	7	0	2	6
Average significant flooding coefficients	–5.34	–4.45	–3.58	null	–100.21	–95.58
Number of significant drought coefficients	0	0	1	0	0	0
Average significant drought coefficients	null	null	–2.451	null	null	null

At the district-level scale, the *SAPEI*-based model performed obviously more preferably than the *SPEI*-based model, as demonstrated by the much greater number of significant regression models in terms of various significance levels, as well as the higher averaged R^2 value in these districts (Figure 10). From Figure 10, it was first found that the significant regression coefficients of both the flooding and drought indices were negative, reconfirming that the intensities of regional drought and flooding were negatively related to cotton climatic yield. More importantly, the yield-reducing effect of cotton flooding was found to be significant in 7 of the 11 study districts. In comparison, the association between cotton drought intensity and cotton climatic yield was poor at the district level.

The growth-stage effect was another item included in investigating the yield-reducing effects of cotton flooding and drought. Therefore, we further established multiple regression relationships between the provincial cotton climatic yield (Y_{cl}) and the corresponding $SESAPEI_{FL}$ (or $SESAPEI_{DR}$) at the four cotton growth stages ($X1$, $X2$, $X3$, and $X4$) to compare the different yield-reducing effects of cotton flooding (or drought) at various growth stages. However, after the entire $SESAPEI_{DR}$ was divided into four growth stages, the specific regression model of drought indices *vs.* cotton climatic yield was not significant. As a result, no further analysis concerning the growth-stage effect in cotton drought reducing climatic yield was performed. In sharp contrast, the specific regression model of cotton climatic yield *vs.* the flooding indices at different stages was particularly significant:

$$Y_{cl} = -1.793X_{FL-Se} + 0.293X_{FL-Bu} - 7.014X_{FL-Fl} - 2.852X_{FL-Bo} + 113.68 \quad (R^2 = 0.389,\ p < 0.05) \tag{16}$$

where, X_{FL-Se}, X_{FL-Bu}, X_{FL-Fl}, and X_{FL-Bo} are the $SESAPEI_{FL}$ at the seedling, budding, flowering and boll-forming, and boll-opening stages, respectively. It is apparent that after the growth stages were considered, only the yield-reducing effect at the flowering and boll-forming stage was significant. Afterward, we excluded the disturbance of the nonsignificant variables by using the stepwise regression method, and the obtained best-fit regression model can be expressed as:

$$Y_{cl} = -7.450X_{FL-Fl} + 80.117 \quad (R^2 = 0.338,\ p < 0.001) \tag{17}$$

From Equation (17), it can be concluded that for the entire Hubei region, cotton-flooding intensity during flooding at the flowering and boll-forming stage can best explain the variation in cotton climatic yield. To examine this conclusion at the district level, we performed stepwise regression analysis for all study districts; the results are listed in Table 4.

Table 4 Best regression models concerning cotton flooding at different growth stages by using stepwise regression

District	Best regression models	R^2	n	p-value
Huangshi	y=-7.051X_{FL-Bo}+75.800	0.221	30	<0.01
Jingzhou	y=-4.906X_{FL-Fl}+50.721	0.182	30	<0.05
Xiangfan	y=-3.482X_{FL-Fl}+33.587	0.150	30	<0.05
Jingmen	y=-4.111X_{FL-Fl}+50.261	0.187	30	<0.05
Xiaogan	y=-6.280X_{FL-Fl}+58.265	0.232	30	<0.01
Xianning	y=-5.424X_{FL-Fl}+69.028	0.276	30	<0.01

Note: X_{FL-Fl} and X_{FL-Bo} represent the flooding index $SESAPEI_{FL}$ at the flowering and boll-forming stage and the boll-opening stage, respectively. Only the districts with significant regression models are displayed here.

From Table 4, it is reconfirmed that the impact of cotton flooding at the flowering and boll-forming stage was much larger than that at other growth stages. In addition, the boll-opening stage had one district with a significant regression model, indicating that cotton flooding during this period may also induce a significant reduction in cotton yield at some sites.

4 Discussion

4.1 The performance of the *SAPEI*

Monitoring flooding and drought regarding agricultural elements is of great importance for agricultural safety, especially under the context of increasing climate change. Currently, the *SPEI* is a popular meteorological index that accounts for crop evapotranspiration and has proven to be satisfactory in monitoring agricultural drought and flooding in many cases[12,21,39,41]. In this study, we adopted the *SAPEI*, an improved index derived from the *SPEI*, to precisely describe cotton flooding and drought, especially accounting for short-term events. Moreover, we specifically compared these two indices in describing the yield-reducing impacts of cotton flooding and drought. Our results in Figure 9 indicate that the *SAPEI*-based regression model (R^2=0490, p<0.001) apparently outperformed the *SPEI*-based regression model (R^2=0.278, p<0.05). In addition, when these regression relationships were further examined for every study district (Figure 10), the preferable performance of the *SAPEI*-based model was reconfirmed, as expected. Hence, it is believed that the *SAPEI* is more efficient than the *SPEI* in describing the yield-reducing impacts of flooding and drought. This discrepancy can be mainly attributed to the fact that the *SPEI* cannot capture short-term cotton drought and flooding, but these contrasting water conditions probably offset each other. In comparison, the *SAPEI* can identify daily flooding and drought and can accumulate them over a given period. In regard to cotton responses to water disasters, the necessity of including short-term flooding and drought has been documented in previous experimental research[4,9,27], in which flooding or drought treatments lasting 2-6 d can induce significant losses in cotton yield. Another possible result of disregarding short-term drought in the *SPEI* can be illustrated by the regression coefficients in Equations (14) and (15): the significant yield-reducing effect of cotton drought was detected by the *SAPEI*-based model but not by the *SPEI*-based model because the *SPEI*-based model underestimated the drought intensity over a certain period after disregarding short-term drought. In addition to the abovementioned difference in calculation steps between the two indices, compared with the *SPEI*, the *SAPEI* replaced the original reference crop evapotranspiration (ET_0) with cotton potential evapotranspiration (cotton ET_c). This modification can be used for crop-specific research, which allows an agrometeorological index to better describe the field moisture conditions at different crop growth phases[44].

4.2 Characteristics of cotton flooding and drought in Hubei

Hubei is located in the subtropical monsoon climate zone and receives abundant rainfall; as a result, flooding-induced waterlogging stress is a major restriction on local crop yield[45]. Our results reconfirmed this opinion: cotton flooding was severe and widespread throughout Hubei (Figure 7a), especially in comparison with cotton drought (Figure 7b). In addition, the flooding-prone and drought-prone areas in Hubei were very different; the former was mainly in northeastern Hubei, while the latter was mainly in southwestern Hubei (Figure 7). A related study[12] employed the *SPEI* to characterize cotton waterlogging proneness in Hubei, in which northeastern Hubei was also identified as the most waterlogging-prone region. This consistent result is not surprising because the *SAPEI* and *SPEI* are generally based on the same theory for identifying water conditions.

To date, although related studies have rarely been performed at the regional level, they have received considerable attention at the field scale. Cotton is widely recognized as a flooding-sensitive crop[4,12,26], and many field experiments have reported that a flooding event lasting very few days (> 2 d) can induce significant yield losses[27,28]. In comparison, cotton is considered relatively tolerant to drought conditions, based on which cotton deficit irrigation has been developed[46,47]. Moreover, the yield-reducing effect of cotton flooding and drought was specifically compared in a field experiment, and the yield-reducing impact of cotton flooding was found to be greater than that of cotton drought[27]. In this study, according to the results obtained from regression models, the yield-reducing effect of cotton flooding was particularly greater than that of cotton drought, despite the employed indices and the studied districts (Equations (14) and (15); Table 3). In this regard, our regional-level results are in line with the abovementioned field experimental studies. It should also be noted that for the present work and other regional-level agrometeorological research, some limitations are difficult to avoid. For instance, irrigation and drainage practices are often disregarded, and only the influences of flooding and drought disasters are accounted for[1].

4.3 The growth-stage effect in cotton flooding and drought

Since the distribution of precipitation varies greatly between cotton growth stages, in this study, the proneness of cotton flooding and drought at different cotton growth stages was quantified after excluding the influence of growth stage durations. The results indicated that the most flooding-prone stage was the flowering and boll-forming stage, and the most drought-prone stage was the budding stage (Figure 5c, Figure 6b). A relevant previous study also evaluated cotton-flooding proneness in the same study region but by using another two indices (i.e., sum of excessive rainfall amount (*SER*) and sum of excessive *SPEI*[12]). However, in that study, the budding stage was identified as the most flooding-prone cotton growth stage. This difference is mainly because applying different indices can result in different conclusions[12]. Specifically, the *SER* merely focuses on the excessive intensity of daily precipitation (even incapable of describing drought intensity); the *SESPEI* describes the overall flooding or drought conditions over a relatively long duration; and the *SESAPEI* focuses on short-term flooding and drought and additionally considers the carry effect of previous soil moisture.

In addition to the abovementioned flooding and drought proneness, the corresponding yield-reducing effects at different growth stages are also noteworthy. Since our regression models based on the drought indices at different growth stages were not significant, the growth-stage effect in drought-reducing cotton climatic yield was not further explored. For cotton flooding, as fully demonstrated by the results at the provincial level (Equation (16)) and district level (Table 4), the yield-reducing effect of cotton flooding at the flowering and boll-forming stage was dramatically greater than that at the other three stages. Hence, it is concluded that the flowering and boll-forming stage is the period during which cotton is most vulnerable to flooding. This conclusion is consistent with the results from previous cotton field experimental studies in which various cotton growth stages were considered and compared[28,48]. The flowering and boll-forming stage is a critical reproductive period for cotton fruit development; during this stage, flooding-induced waterlogging stress not only reduces dry matter

accumulation but also reduces the number of cotton bolls[27], which directly results in a severe reduction in cotton yield. However, it should be noted that the division of cotton growth stages in this work disregards the difference between sites and years. In addition to agricultural management, climatic factors also affect the length of specific cotton growth stages; hence, the rough division of crop growth stages is a deficiency of this work. Similarly, in many previous regional-scale analyses concerning crop drought and flooding disasters, the division of growth stages was usually rough (i.e., disregarding spatial and temporal differences) and even on a monthly timescale[12,24,41,49]. In the above studies, the rough division of crop growth stages is mainly because of limited available grow-stage-relevant data in different study sites and years. For this concern, Yao et al.[49] performed a specific discussion in a recent work and suggested that growth stage simulation models as well as more specific datasets for growth stages can be employed in future relevant work.

4.4 Suggestions for irrigation and drainage

Regional analysis of cotton flooding and drought can provide useful suggestions for local irrigation and drainage. Our results indicated that both the proneness and yield-reducing effect of cotton flooding were very great in Hubei, much greater than those of cotton drought (Figure 7 and Table 3). In Hubei, cotton is easily confronted with flooding due to poor drainage capacity and perched water tables. In comparison, the impact of cotton drought was relatively slight because of various factors, such as cotton drought tolerance and the low intensity of cotton drought. However, the *SAPEI*-based model also revealed that, at the provincial level, both cotton flooding and drought had negatively significant impacts on cotton climatic yield. This finding suggested that not only drainage practices but also irrigation practices are in urgent need of improvement. In addition, specific schedules for cotton irrigation and drainage should depend on growth stages. Our results suggested that the flowering and boll-forming stage was the most flooding-prone period (Figure 5); in addition, cotton at this stage was also most vulnerable to flooding (Equation (16)). Hence, efficient field drainage during the flowering and boll-forming stage should be the primary goal.

Crop-water relations are important issues in agricultural research. For the benefit of scheduling irrigation and drainage, crop-water production functions (i.e., the quantitative relationships between crop yield and water stress intensity)[50,51] are extensively developed to simulate crop yield responses to various water stress conditions. In this work, the relationships of cotton climatic yield *vs.* cotton flooding and drought intensity were established, which can be applied to predict regional cotton climate-induced yield. The *SAPEI*-based regression model can significantly (R^2=0.49, p<0.001) explain the variation in provincial cotton climatic yield; its simulations matched the actual climatic yield (Figure 9). In the future, when more agrometeorological factors, e.g., air temperature and humidity, are included, more comprehensive and precise prediction models will be obtained.

5 Conclusions

Flooding and drought are major natural disasters worldwide, posing severe threats to agricultural safety. Studying the patterns and yield-reducing effects of flooding and drought with special regard to crop growth stages can provide valuable guidance for irrigation and drainage scheduling. By employing a daily step agrometeorological index named *SAPEI*, this work successfully revealed the specific spatiotemporal patterns of cotton flooding and drought at different cotton growth stages in Hubei; more importantly, through the established regression models for cotton climatic yield simulation, the yield-reducing impacts of cotton flooding and drought regarding growth stages were determined and compared. In summary, this study provides a valuable reference for irrigation and drainage in cotton fields and provides new insights into the response of cotton to flooding and drought at a regional level. The results mainly showed that the proneness of cotton flooding was much greater than that of drought. The flowering and boll-forming stage was the most flooding-prone period, while the budding stage was the most drought-prone period. Northeastern Hubei and southwestern Hubei were the most flooding-prone and drought-prone areas, respectively. In addition, the *SAPEI* was efficient in describing the negative impacts of flooding and drought on cotton climatic yield, obviously outperforming the *SPEI*. The *SAPEI*-based regression model revealed that both cotton flooding and drought had significant negative impacts on provincial cotton climatic yield over the past six decades. However, the impact of cotton flooding was much greater than that of cotton drought, as fully demonstrated by the regression results corresponding to different indices and various study districts. Moreover, when cotton growth stages were considered in the regression analysis, it was suggested that cotton flooding during the flowering and boll-forming stage was most noteworthy since its impact on cotton climatic yield was most significant at both the province level and district level. In conclusion, the *SAPEI* is a powerful tool for monitoring crop drought and flooding; cotton flooding is the dominant water disaster for Hubei cotton, especially during the flowering and boll-forming stage and in northeastern Hubei.

Acknowledgements

This research was financially supported by the National Natural Science Foundation of China (Grant No. 51861125203, U1911204, and 51909286), and the National Key R&D Program of China (Grant No. 2021YFC3001000 and 2018YFC1508301).

[References]

[1] Shi W J, Wang M L, Liu Y T. Crop yield and production responses to climate disasters in China. Science of The Total Environment, 2021; 750: 141147.

[2] Kaur G, Singh G, Motavalli P P, Nelson K A, Orlowski J M, Gloden B R. Impacts and management strategies for crop production in waterlogged or flooded soils: A review. Agronomy Journal, 2020; 112: 1475–1501.

[3] Xing Z X, Yang Z R, Fu Q, Li H, Gong X L, Wu J Y. Characteristics and risk assessment of agricultural meteorological disasters based on 30 years' disaster data from Heilongjiang Province of China. Int J Agric & Biol Eng, 2017; 10(6): 144–154.

[4] Zhang Y J, Chen Y Z, Lu H Q, Kong X Q, Dai J L, Li Z H, et al. Growth, lint yield and changes in physiological attributes of cotton under temporal waterlogging. Field Crops Research, 2016; 194: 83–93.

[5] Shaw R E, Meyer W S, McNeill A, Tyerman S D. Waterlogging in Australian agricultural landscapes: a review of plant responses and crop models. Crop & Pasture Science, 2013; 64(6): 549–562.

[6] Ullah A, Sun H, Yang X, Zhang X L. Drought coping strategies in cotton: increased crop per drop. Plant Biotechnology, 2017; 15: 271–284.

[7] Wang R, Ji S, Zhang P, Meng Y L, Wang Y H, Chen B L, et al. Drought effects on cotton yield and fiber quality on different fruiting branches. Crop Science, 2016; 56: 1265–1276.

[8] Pettigrew W T. Physiological consequences of moisture deficit stress in cotton. Crop Science, 2004; 44(4): 1265–1272.

[9] Niu J, Zhang S P, Liu S D, Ma H J, Chen J, Shen Q, et al. The compensation effects of physiology and yield in cotton after drought stress. Journal of Plant Physiology, 2018; 224: 30–48.

[10] Thieken A H, MLler M, Kreibich H, Bruno Merz. Flood damage and influencing factors: wew insights from the August 2002 flood in Germany.

Water Resources Research, 2005; 41: W12430.
[11] Wei Y Q, Jin J L, Cui Y, Ning S W, Fei Z Y, Wu C G, et al. Quantitative assessment of soybean drought risk in Bengbu city based on disaster loss risk curve and DSSAT. International Journal of Disaster Risk Reduction, 2021; 56: 102126.
[12] Qian L, Chen X H, Gao Y W, Deng K N, Wang X G, Zeng W Z, et al. Quantifying the impacts of waterlogging on cotton at different growth stages: A case study in Hubei Province, China. Agronomy Journal, 2021; 113: 1831–1851.
[13] Wu H, Michael J H, Albert W, Qi H. An evaluation of the standardized precipitation index, the China-Z index and the statictical Z-score. International Journal of Climatology, 2001; 21: 745–758.
[14] McKee T B, Doesken N J, Kleist J, The relationship of drought frequency and duration to time scales. In Proceedings of the Eighth Conference on Applied Climatology, Boston, 1993; pp.179-184.
[15] Cai G Q, Chen S J, Liu Y, Sun H W, Chen C Q, Gui D W, et al. Using multiple indexes to analyze temporal and spatial patterns of precipitation and drought in Xinjiang, China. Theoretical and Applied Climatology, 2020; 142: 177–190.
[16] Vicente-Serrano S M, Beguería S, López-Moreno J I. A multiscalar drought index sensitive to global warming: the standardized precipitation evapotranspiration index. Journal of Climate, 2010; 23: 1696–1718.
[17] Starks P J, Steiner J L, Neel J P S, Turner K E, Northup B K, Gowda P H, et al. Assessment of the standardized precipitation and evaporation index (SPEI) as a potential management tool for grasslands. Agronomy, 2019; 9: 235.
[18] Polong F, Chen H S, Sun S L, Ongoma V. Temporal and spatial evolution of the standard precipitation evapotranspiration index (SPEI) in the Tana River Basin, Kenya. Theoretical and Applied Climatology, 2019; 138: 777–792.
[19] Raja R, Nayak A K, Panda B B, Lal B, Tripathi R, Shahid M, et al. Monitoring of meteorological drought and its impact on rice (Oryza sativa L.) productivity in Odisha using standardized precipitation index. Archives of Agronomy and Soil Science, 2014; 60: 1701–1715.
[20] Huang J, Zhang F M, Xue Y, Li Q. Recent changes of extreme dryness/wetness pattern and its possible impact on rice productivity in Jiangsu Province, southeast China. Natural Hazards, 2018; 84: 1967–1979.
[21] Zhou Z Q, Shi H Y, Fu Q, Li T X, Gan T Y, Liu S N. Assessing spatiotemporal characteristics of drought and its effects on climate-induced yield of maize in Northeast China. Journal of Hydrology, 2020; 558: 125097.
[22] Guo E L, Liu X P, Zhang J Q, Wang Y F, Wang C L, Wang R, et al. Assessing spatiotemporal variation of drought and its impact on maize yield in Northeast China. Journal of Hydrology, 2017; 553: 231–247.
[23] Li C, Wang R H, Xu J X, Luo Y J, Tan M L, Jiang Y L. Analysis of meteorological dryness/wetness features for spring wheat production in the Ili River basin, China. International Journal of Biometeorology, 2018; 62: 2197–2204.
[24] Gao C, Yin Z X, Xu Y. Space-time characteristics of drought and flood in main growing periods of winter wheat in Huaihe River Basin and its impact on yield. Transactions of the CSAE, 2017; 33: 101–111. (in Chinese)
[25] Chen X C, Li Y, Yao N, Liu D L, Javed T, Liu C C, et al. Impacts of multi-timescale SPEI and SMDI variations on winter wheat yields. Agricultural Systems 2020; 185, 102955.
[26] Najeeb U, Bange M P, Tan D K Y, Atwell B J. Consequences of waterlogging in cotton and opportunities for mitigation of yield losses. AoB Plants 2015; 7: plv080.
[27] Qian L, Chen X H, Wang X G, Huang S, Luo Y Y. The effects of flood, drought, and flood followed by drought on yield in cotton. Agronomy, 2020; 10: 555.
[28] Wang X S, Zhong D, Zhang W Z, Meng Z J, Xiao C, Lv M C. Effect of waterlogging duration at different growth stages on the growth, yield and quality of cotton. PloS one, 2017; 12(1): e0169029.
[29] Wu H, Wang X G, Xu M, Zhang J X. The effect of water deficit and waterlogging on the yield components of cotton. Crop Science, 2018; 58(4): 1751–1761.
[30] Liu S M, Wang H, Yan D H, Qin T L, Wang Z L, Wang F X. Crop growth characteristics and waterlogging risk analysis of Huaibei Plain in Anhui Province, China. Journal of Irrigation & Drainage Engineering, 2017; 143: 04017042.
[31] Dai J L, Dong H Z. Intensive cotton farming technologies in China: Achievements, challenges and countermeasures. Field Crops Research, 2014; 155: 99–110.
[32] Han W R, Liu S L, Wang J, Lei Y P, Zhang Y J, Han Y C, et al. Climate variation explains more than half of cotton yield variability in China. Industrial Crops and Products, 2022; 190: 115905.
[33] Li J, Wang Z L, Wu X S, Xu C Y, Guo S L, Chen X H. Toward monitoring short-term droughts using a novel daily scale, standardized antecedent precipitation evapotranspiration index. Journal of Hydrometeorology, 2020; 21: 891–908.
[34] Chen J H, Yu W G, Liu R N, Yue W, Chen X. Daily standardized antecedent precipitation evapotranspiration index (SAPEI) and its adaptability in Anhui Province. Chinese Journal of Eco-Agriculture, 2019; 27: 919–928. (in Chinese)
[35] Doorenbos J, Pruitt W O, Crop water requirements. FAO. Irrigation and drainage paper no. 24. FAO: Rome, Italy, 1977.
[36] Allan R G, Pereira L S, Raes D, Smith M. Crop evapotranspirationm guidelines for computing crop water requirements-FAO Irrigation and drainage paper 56. FAO 1998; 56p.
[37] Shaw R E, Meyer W S. Improved empirical representation of plant responses to waterlogging for simulating crop yield. Agronomy Journal, 2015; 107(5): 1711–1723.
[38] Liu Y J, Chen J, Pan T. Spatial and temporal patterns of drought hazard for China under different RCP scenarios in the 21st century. International Journal of Disaster Risk Reduction, 2021; 52: 101948.
[39] Wang Z L, Huang Z Q, Li J, Zhong R D, Huang W W. Assessing impacts of meteorological drought on vegetation at catchment scale in China based on SPEI and NDVI. Transactions of the CSAE, 2016; 32(14): 177–186. (in Chinese)
[40] Yuan Y, Yan D H, Yuan Z, Yin J, Zhao Z N. Spatial distribution of precipitation in Huang-Huai-Hai River Basin between 1961 to 2016, China. International Journal of Environmental Research and Public Health, 2019; 16: 3404.
[41] Tian L Y, Yuan S S, Quiring S M. Evaluation of six indices for monitoring agricultural drought in the southcentral United States. Agricultural & Forest Meteorology, 2018; 249: 107–119.
[42] Mistry P, Bora G. Development of yield forecast model using multiple regression analysis and impact of climatic parameters on spring wheat. Int J Agric & Biol Eng, 2019; 12(4): 110–115.
[43] Thiagarajan A, Lada R R, Muthuswamy S, Adams A. Agroclimatology-based yield model for carrot using multiple linear regression and artificial neural networks. Agronomy Journal, 2013; 105(3): 863–873.
[44] Pei W, Fu Q, Liu D, Li T X. A drought index for rainfed agriculture: the standardized precipitation crop evapotranspiration Index (SPCEI). Hydrological Processes, 2019; 33: 803–815.
[45] Chen Y Y, Huang J F, Song X D, Wu H Y, Sheng S X, Liu Z X, et al. Waterlogging risk assessment for winter wheat using multi-source data in the middle and lower reaches of Yangtze River. International Journal of Agricultural and Biological Engineering, 2018; 11: 198–205.
[46] Basal H, Dagdelen N, Unay A, Yilmaz E. Effects of deficit drip irrigation ratios on cotton (Gossypium hirsutum L.) yield and fibre quality. Journal of Agronomy & Crop Science, 2009; 195: 19–29.
[47] Li H F, Qi Z M, Gui D W, Zeng F J. Water use efficiency and yield responses of cotton to field capacity-based deficit irrigation in an extremely arid area of China. International Journal of Agricultural and Biological Engineering 2019; 12, 91-101.
[48] Qian L, Wang X G, Luo Y Y, Sun H W, Luo W B. Responses of cotton at different growth stages to aeration stress under the influence of high temperature. Crop Science, 2018; 58(1): 342-353.
[49] Yao P, Qian L, Wang Z L, Meng H Y, Ju X L. Assessing drought, flood, and high temperature disasters during sugarcane growth stages in Southern China. Agriculture, 2022; 12: 2117.
[50] Tarkalson D D, King B A, Bjorneberg D L. Yield production functions of irrigated sugarbeet in an arid climate. Agricultural Water Management, 2018; 200: 1–9.
[51] Wang K, Yuan X J, Cao X Q, Xue Y F. Experimental study on water production function for waterlogging stress on corn. Procedia Engineering, 2012; 28: 598–603.